

1. Motivation

One of the many challenges that we face in wireline telemetry is how to operate high-speed data transmissions over non-ideal, poorly controlled media. The key to any telemetry system design depends on the system's ability to adapt to a changing environment. While adaptive equalization can account for frequency-dependent cable attenuation by inverting channel distortion [Campbell 96, pp. 68], there still exists the need to reduce other sources of noise, for example, the near-end crosstalk (NEXT) that exists in a multiconductor cable. Typically, a multiconductor cable is used as a medium in a wireline telemetry system for two reasons:

1. Multiple cables increase the number of communication channels and therefore increase the total operating bandwidth of the system.
2. In addition to data cables, a power cable is needed to supply electricity to the telemetry transmitter at the remote end.

The principal source of interference is now the coupling between the power cable and data cable. This noise is far from white and can reduce the SNR by more than 10 dB, an amount that can severely hamper the telemetry system's performance.

The structure of the paper is as follows. First we discuss the observed periodic non-Gaussian noise and explain why it is difficult to reduce this noise using frequency domain filtering. Next, we introduce an innovative time domain approach, Active Noise Cancellation, that can reduce in-band crosstalk without distorting the signal of interest. Finally, we outline the specification of this cancellation algorithm using a homogeneous synchronous dataflow (HSDF) graph and describe its implementation on an embedded DSP processor.

2. Periodic non-Gaussian noise

The crosstalk interference can be described as a collection of noise pulses superimposed on top of a slow varying 60 Hz sine wave originated from the power supply.

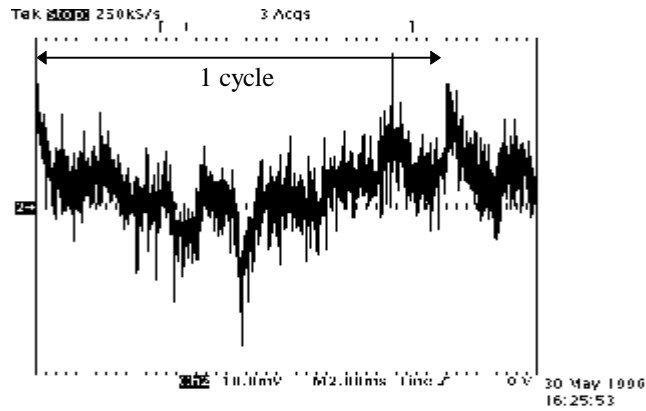


Figure 1. Oscilloscope capture of approximately one cycle of crosstalk.

Figure 1 is an oscilloscope capture of the actual crosstalk interference. The double arrow line above the figure approximately marks one period of the 60 Hz crosstalk. To better describe the effective noise, we can decouple the crosstalk into a 60 Hz sine component and a collection of periodic noise pulses as seen in Figure 2.

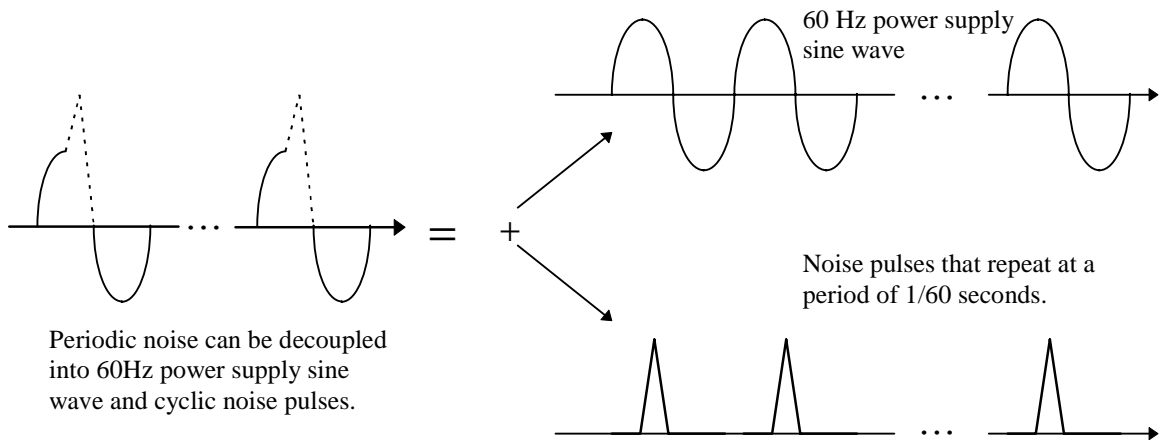


Figure 2. Decoupling of crosstalk into a 60 Hz sine component and periodic noise pulses.

Each of the noise pulses in Figure 2 is a collection of impulses as shown in Figure 3(a). Hence the crosstalk creates a non-Gaussian noise, because the noise is periodic, that maps to a wideband noise in the frequency domain, because the noise consists of impulses in the time domain. The wideband noise completely overlaps the transmitted QAM signal which has a bandwidth of, for example, $f_b = 70\text{ kHz}$ and is modulated by a carrier of $f_c = 52.5\text{ kHz}$, as seen in Figure 3(b).

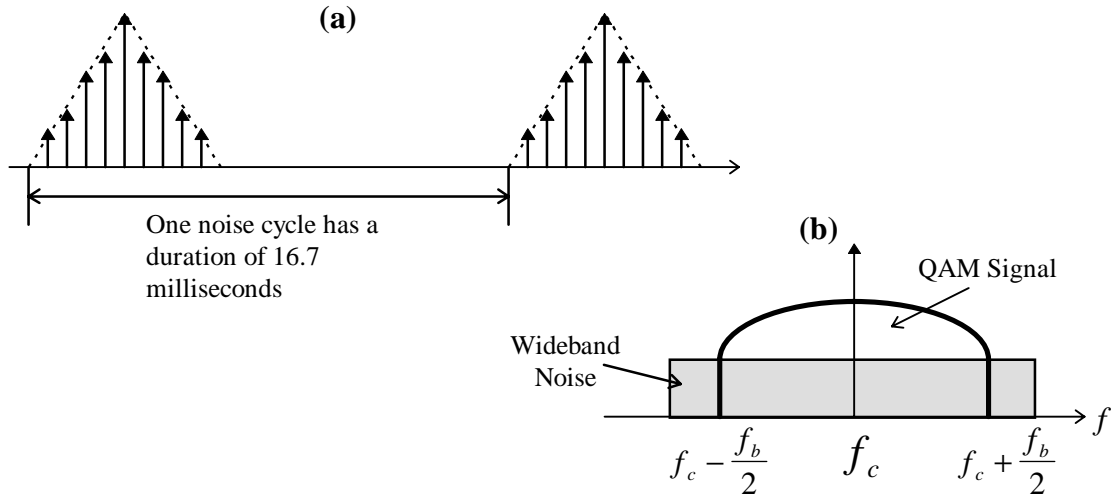


Figure 3. (a) Each 60 Hz noise cycle consists of a group of sampled impulses. (b) QAM signal with overlapping wideband noise.

As a result, frequency domain filters cannot remove the wideband noise without actually removing the desired QAM signal as well and frequency domain filtering becomes an ineffective approach to eliminating the periodic crosstalk noise.

3. Quadrature Amplitude Modulation

Quadrature Amplitude Modulation avoids the spectral inefficiency of Double Sideband Amplitude Modulation by mapping a stream of bits onto a constellation and modulating the coordinates of the constellation with two orthogonal carriers 90° apart in phase. Thus, the transmitted signal is

$$s(t) = x_p(t) \cos(\omega_c t) - x_q(t) \sin(\omega_c t)$$

At the receiver end, $s(t)$ is multiplied by $\cos(\omega_c t)$ and $-\sin(\omega_c t)$ to recover the original data, the products are

$$y_p(t) = x_p(t) \cos^2 \omega_c t - x_q(t) \sin \omega_c t \cos \omega_c t = \frac{x_p(t)(1 + \cos 2\omega_c t) - x_q(t) \sin 2\omega_c t}{2}$$

$$y_q(t) = -x_p(t) \cos \omega_c t \sin \omega_c t + x_q(t) \sin^2 \omega_c t = \frac{x_p(t) \sin 2\omega_c t + x_q(t)(1 - \cos 2\omega_c t)}{2}$$

The sidebands of the second harmonics of the carriers are then removed by low-pass filtering, and the receiver baseband signals $y_p(t)$ and $y_q(t)$ are then within a factor 2 to the originals [Campbell 96, pp. 26-53].

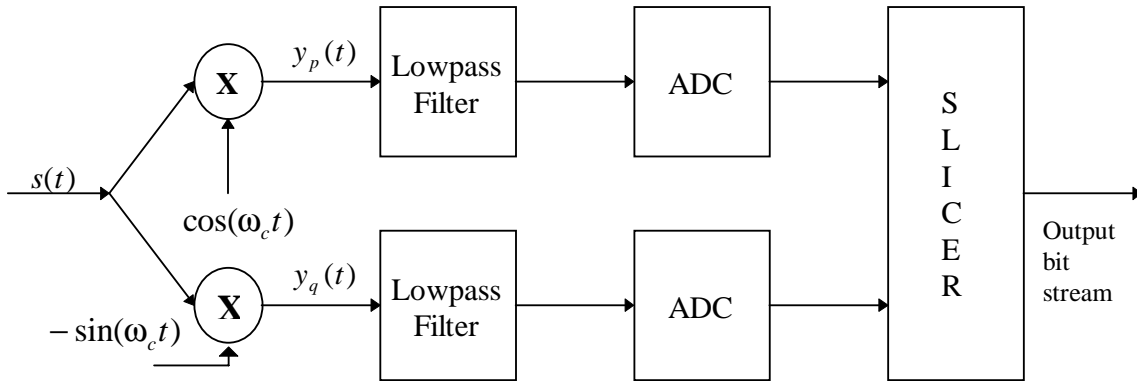


Figure 4. QAM Receiver Structure.

Figure 4 illustrates a QAM receiver. It is clear that intense computation is needed to multiply $s(t)$ with the carriers and to lowpass filter the resulting signals $y_p(t)$ and $y_q(t)$. To reduce unnecessary computation, Schlumberger developed and patented a technique that eliminates the need for signal reconstruction.

4. Existing Noise Cancellation Techniques

Early research has been done in the noise cancellation area. The most famous work is perhaps the Least Mean Square Algorithm, illustrated in Figure 5, introduced by Widrow and Hoff [Widrow 75] in the mid 70s. However, the LMS algorithm presented by Widrow was aimed at removing single tone interference and not

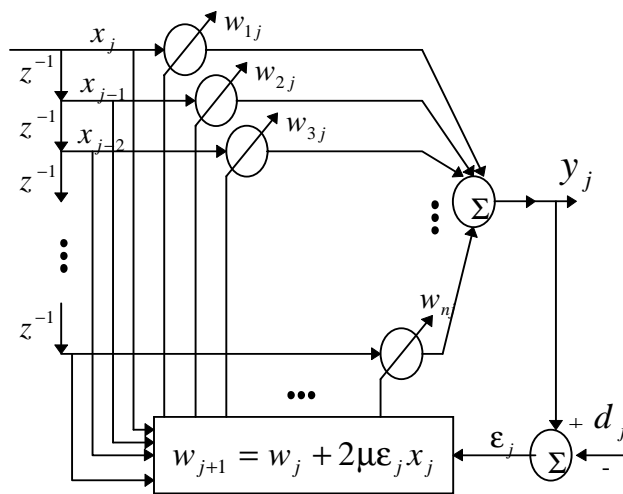


Figure 5. Widrow-Hoff LMS Algorithm.

periodic wideband noise.

5. Active Noise Cancellation

The idea of noise cancellation is to collect an estimation of the periodic wideband noise during receiver training. The collected noise estimate is then subtracted from the received QAM signal during steady state data transmission. Figure 6 is a block representation of the receiver operation during training.

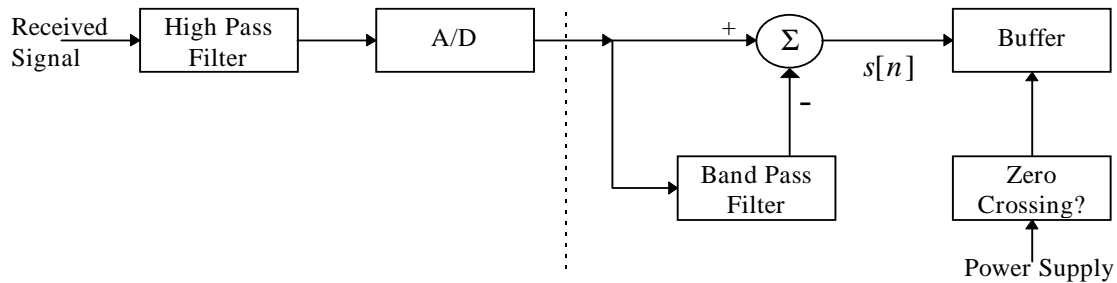


Figure 6. Block diagram of receiver operation during training.

The structure to the right of the dash line is responsible for noise extraction. The transmitted signal is known during receiver training, for example, the signal can be a 52.5 kHz tone. It is clear that with the transmitted signal known a priori, noise estimate can be computed as

$$\text{Noise Estimate} \equiv s[n] = \text{Actual received signal} - \text{Training signal} .$$

Furthermore, the training signal can be extracted at the receiver using a narrow band notch filter centered at the carrier frequency 52.5 kHz. The notch filter is implemented using a second-order IIR biquad with the following transfer function.

$$\frac{Y(z)}{S(z)} = \frac{k_0(1 - z^{-1})}{1 - k_1z^{-1} - k_2z^{-2}}$$

Equation 1. Notch filter transfer function.

The filter structure is illustrated in Figure 7. The coefficients k_0 , k_1 , and k_2 can be adjusted to obtain the desired filter sharpness and filter build-up time.

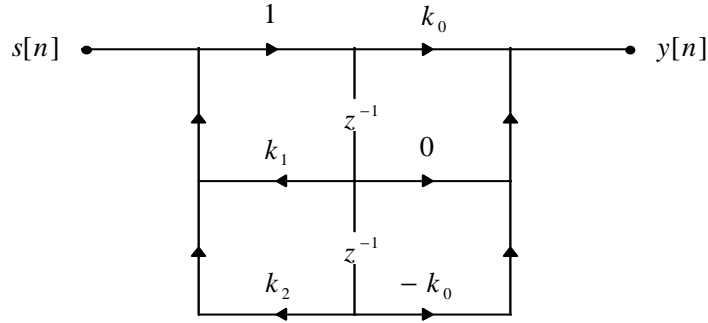


Figure 7. IIR biquad bandpass filter.

The buffer block in Figure 6 can be implemented using a circular buffer and updated using the following formula. The variable i represents the i th sample in the 60 Hz noise cycle.

$$\begin{aligned} buffer_i[n] &= \frac{\alpha}{\beta} s[n] + (1 - \frac{\alpha}{\beta}) buffer_i[n-1] \\ &= \frac{\alpha}{\beta} \left[\sum_{k=0}^{N-1} (1 - \frac{\alpha}{\beta})^k s[n-k] \right] \end{aligned}$$

Equation 2. Buffer update equation.

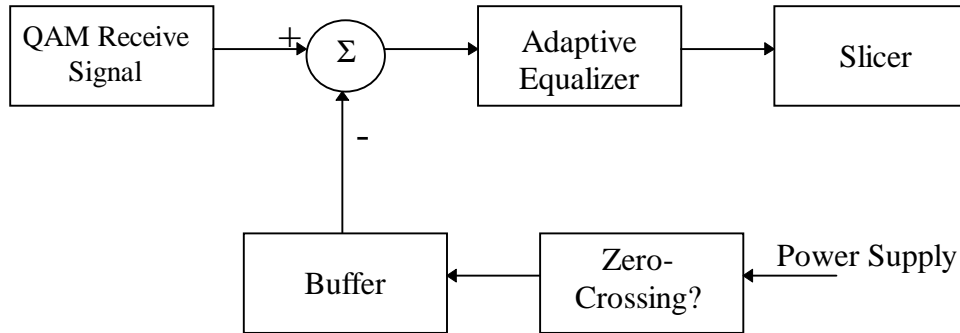
N is the number of 60 Hz noise cycles during training duration. The ratio α/β is the buffer update factor and must be chosen carefully to optimize the cancellation algorithm. From Equation 2, it is clear that if the update factor is zero, then no update is made to the noise buffer and it retains its initial values. If the factor is one, then only the most current noise cycle is kept. Therefore, an update factor close to zero implies that the noise estimate will be approximately a running average while a factor close to one means that the most recent noise cycle will be weighted more. Averaging is a more conservative approach but the noise estimate will remain valid for a longer duration. On the other hand, an emphasis on more recent noise cycles is an aggressive approach that will produce a better result in the short term in exchange for the need to frequently reacquire the noise pattern which may not be possible during steady state.

The zero-crossing block in Figure 6 is used to combat 60 Hz crosstalk drift. Whenever the positive zero-crossing occurs in the power supply, the zero-crossing block will reset

the buffer pointer to the head of the buffer array, i.e. sample number one of the noise estimate.

Actual noise cancellation occurs in steady state. Figure 8 is a block diagram of the receiver operation during steady state. The noise estimate is subtracted from the received QAM signal sample-by-sample to achieve an improved receiver noise performance.

Figure 8. Noise Cancellation in steady state.



6. Homogeneous Synchronous Dataflow

Synchronous Dataflow (SDF) [Pino 95] is a well-suited model of computation for digital communication systems which often process an endless supply of data. The simplest form of an SDF is a homogeneous SDF graph where the number of tokens consumed and produced on each arc is a constant one. HSDF fits nicely with the specification of our Active Noise Cancellation. Figure 9 illustrates the algorithm using an HSDF graph. The actor firing sequence will be {ADC Read, Int-to-Float, Notch Filter, Estimate Noise, Zero-Crossing, Buffer Write} during training and {ADC Read, Int-to-Float, Cancel Noise, Zero-Crossing} during steady state.

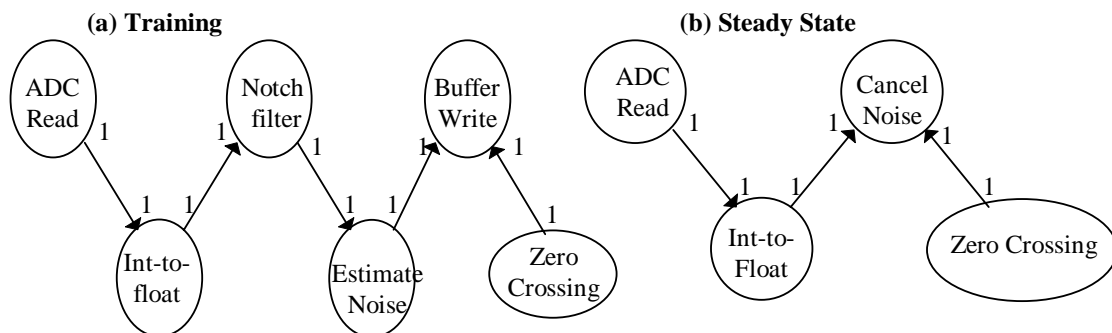


Figure 9. HSDF graph representation of receiver operation in (a) training and (b) steady state.

7. Performance

Active Noise Cancellation has been simulated using Analog Device's SHARC simulator and its performance analyzed using MATLAB. Crosstalk interference is created by appending multiple cycles of the measured noise, seen in Figure 1. Active Noise Cancellation on average improves the Mean Square Error by 7dB as illustrated in Table 1. Also notice from the table that an accurate zero-crossing information is crucial to proper noise cancellation because incorrect cancelling can worsen the noise.

Table 1. Performance of Active Noise Cancellation.

Method	Average MSE	Average SNR
Required values under Gaussian noise to obtain an BER of 10^{-7}	-35 dB	35 dB
No Active Noise Cancellation	-25 dB	25 dB
Active Noise Cancellation <i>without</i> Zero-Crossing information	-23 dB	23 dB
Active Noise Cancellation <i>with</i> Zero-Crossing information	-32 dB	32 dB

8. Conclusion

We have developed an effective Active Noise Cancellation algorithm to improve receiver performance in the presence of non-Gaussian wideband noise. Modeling of ANC using HSDF proves that the algorithm is simple enough to be implemented on most existing DSPs. We plan to show the effectiveness of ANC in a real noise environment and to verify that an average of -32 dB MSE can be obtained while maintaining a BER of 10^{-7} .

9. References

[Campbell 96] Heather A. Campbell, *Simulation of Quadrature Amplitude Demodulation in a Digital Telemetry System*, Master Thesis, Massachusetts Institute of Technology, Feb. 1996.

[Pino 95] Jose Luis Pino, Shuvra S. Bhattacharyya, and Edward A. Lee, "A Hierarchical Multiprocessor Scheduling System for DSP Applications," *Proc. of 29th Asilomar Conf. on Signals, Systems, and Computers*, October 1995.

[Widrow 75] B. Widrow, J.R. Glover, et al., "Adaptive Noise Cancelling: Principles and Applications," *IEEE Proc.*, vol. 63, no.12, pp. 1692-1716, Dec. 1975.